Chemical Insights in the Concept of Hybrid Drugs: The Antitumor Effect of Nitric Oxide-Donating Aspirin Involves A Quinone Methide but Not Nitric Oxide nor Aspirin

Niels Hulsman,[†,‡,§] Jan Paul Medema,[†] Carina Bos,[†] Aldo Jongejan,[‡] Rob Leurs,[‡] Martine J. Smit,[‡] Iwan J. P. de Esch,[‡] Dick Richel,[†] and Maikel Wijtmans*[,‡,§]

Laboratory for Experimental Oncology and Radiobiology, Academic Medical Center, University of Amsterdam, Meibergdreef 9, 1105 AZ Amsterdam, The Netherlands, and Leiden/Amsterdam Center for Drug Research, Division of Medicinal Chemistry, Faculty of Science, Vrije Universiteit Amsterdam, De Boelelaan 1083, 1081 HV Amsterdam, The Netherlands

Hybrid drug **1** (NO-ASA) continues to attract intense research from chemists and biologists alike. It consists of ASA and a −ONO_2 group connected through a spacer and is in preclinical development as an antitumor drug. We report that, contrary to current beliefs, neither ASA nor NO contributes to this antitumor effect. Rather, an unsubstituted QM was identified as the sole cytotoxic agent. QM forms from **1** after carboxylic ester hydrolysis and, in accordance with the HSAB theory, selectively reacts with cellular GSH, which in turn triggers cell death. Remarkably, a derivative lacking ASA and the −ONO_2 group is 10 times more effective than **1**. Thus, our data provide a conclusive molecular mechanism for the antitumor activity of **1**. Equally importantly, we show for the first time that a "presumed invisible" linker in a hybrid drug is not so invisible after all and is in fact solely responsible for the biological effect.

Introduction

Medicinal research is constantly seeking to improve the efficiency of drugs. One approach involves the use of so-called hybrid drugs, which comprises the incorporation of two drug pharmacophores in one single molecule with the intention to exert dual drug action.[1] For example, one of the hybrid parts may be incorporated to counterbalance the known side effects associated with the other hybrid part, or to amplify its effect through action on another biotarget. Some hybrid drugs are designed to interact with multiple targets as one single molecule, and others require prior disintegration to afford the active hybrid components. An archetypical example of the latter class is NO-ASA[a], which consists of ASA and a nitrate group (−ONO_2) as a NO donor connected by a spacer (Scheme 1). Its development was based on the assumption that carboxylic ester hydrolysis would afford ASA and an NO-donating moiety. The resulting advantage is that the known gastrointestinal side effects of ASA would be reduced by this concomitant release of NO (NO-hybrid theory).[2] A possible application for such hybrids is in the area of chemoprevention, because ASA is a known moderately active chemopreventive agent.[3] Two NO-ASA isomers, **1** (*para*-isomer) and **3** (*ortho*-isomer), were indeed found to be highly effective in inhibiting growth of colon cancer both in vitro and in vivo.[4,5] These activities were of such unexpectedly high nature that intensive research on *para*-isomer **1** was initiated. It proved active in a variety of different colon cancer cell lines as well as

* To whom correspondence should be addressed. Phone: +31(0)20-5987603. Fax: +31(0)20-5987610. E-mail: wijtmans@few.vu.nl.
† University of Amsterdam.
‡ Vrije Universiteit Amsterdam.
§ These authors contributed equally.

a Abbreviations: ASA, aspirin; BSO, DL-buthionine(S,R)-sulfoximine; cGMP, cyclic guanosine monophosphate; DFT, density functional theory; EtGSH, GSH ethyl ester; FACS, fluorescence-activated cell sorter; FADD, Fas associated protein with a death domain; GSH, glutathione; HSAB, hard-soft acid-base; iNOS, inducible nitric oxide synthase; MAPK, mitogen-activated protein kinase; NAC, N-acetyl-L-cysteine; NO, nitric oxide; NO-ASA, nitric oxide-donating aspirin; NSAID, nonsteroidal anti-inflammatory drug; PARP, poly(ADP-ribose) polymerase; PI, propidium iodide; QM, quinone methide; SNAP, S-nitroso-N-acetylpenicillamine; Tcf, T-cell factor; ZORA, zeroth-order regular approximation.
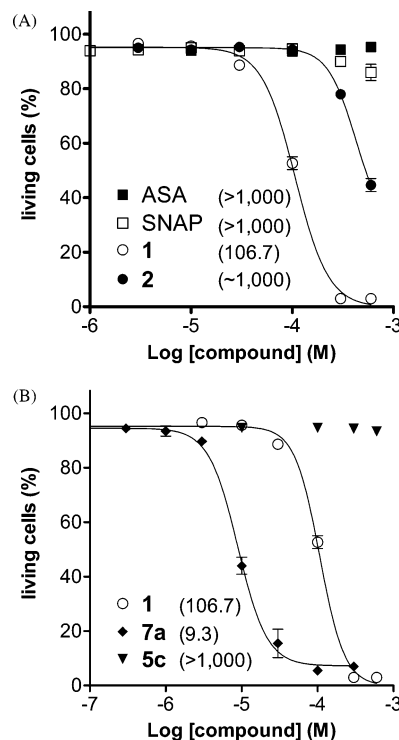

Figure 1. Induction of cell death of HT29 cells after 24 h by (A) reference compounds **1**, **2**, SNAP, and ASA and (B) model compounds **7a** and **5c** lacking the aspirin or nitrate moiety. Cell death was measured using FACS with PI staining, and % living cells is plotted. Results are presented as the mean of three independent experiments, with bars depicting the standard error. The value between parentheses represents the EC50 value in μM for the respective compound.

in other cancer types[6−8] and is in preclinical development as a chemopreventive agent.[9,10] Recently, its potential for use in combination chemotherapy was demonstrated.[11] Among others, MAPK signaling,[9] iNOS expression and activity,[12] and oxidative stress[13,14] are involved in the apoptotic effect of **1**.

However, we reasoned that the induction of apoptosis cannot be explained by a hybrid action because of conflicting mecha-

Scheme 1. Synthetic Sequences for Model Compounds and Structures of SNAP and the Three Isomers **1**−**3** of NO-ASA[a]

a: *para*, R=CH$_3$
b: *para*, R=*t*-Bu
c: *para*, R=2-OAc-Ph
d: *meta*, R=CH$_3$
e: *meta*, R=2-OAc-Ph
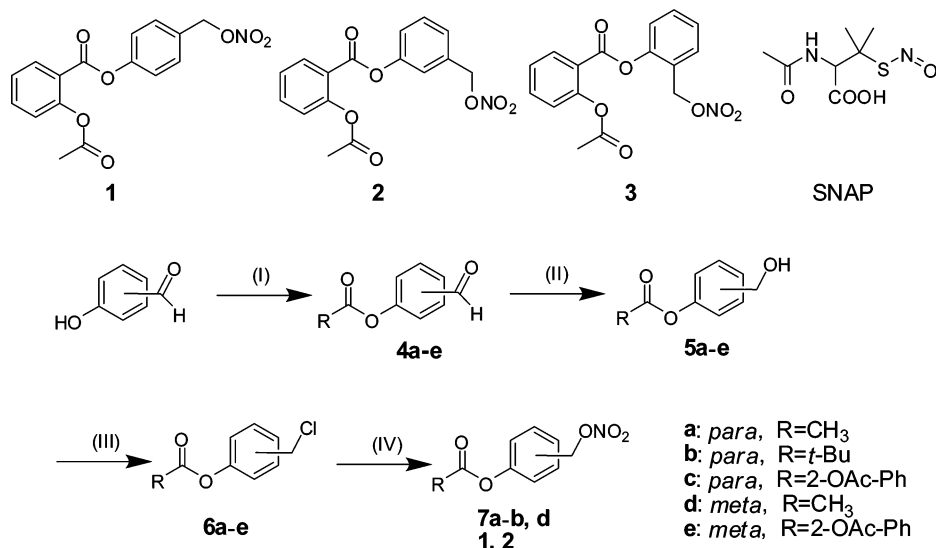
[a] Reagents and conditions: (I) RCOCl, Et$_3$N, THF or DCM, rt, 2−24 h; (II) NaBH$_4$, THF, rt, 2 h; (III) SOCl$_2$, pyridine, toluene or CH$_2$Cl$_2$, rt or reflux, 2−24 h; (IV) AgNO$_3$, CH$_3$CN, reflux, 2−12 h.

Scheme 2. Mechanism of QM Formation for Benzyl Nitrates and Chloride[a]
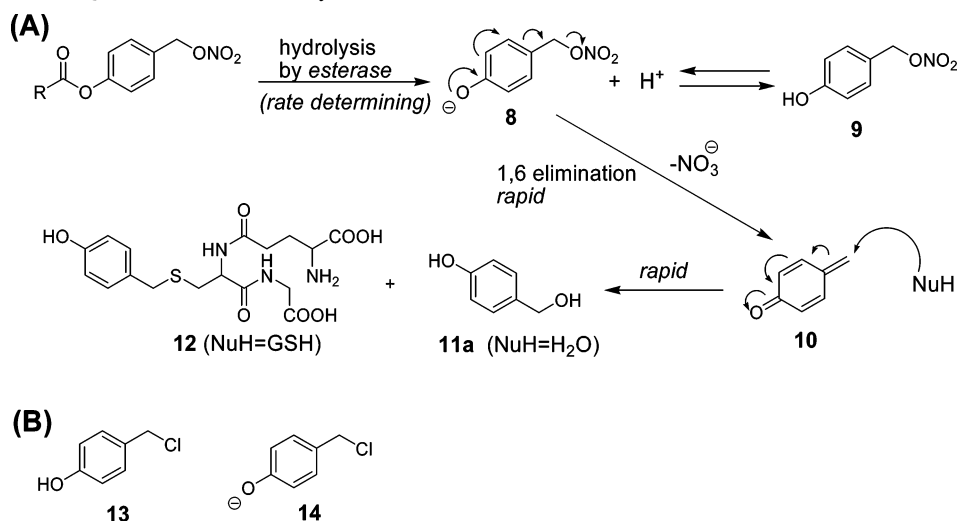
[a] (A) Proposed mechanism of QM formation from **1** or other benzyl nitrates and reaction of this species with cellular nucleophiles GSH and H$_2$O. NuH = nucleophile. (B) The QM formation from substituted benzyl chlorides is identical to the mechanism depicted in (A), but with **13** and **14** instead of **9** and **8**, respectively.
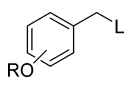
nistic results in the literature. For example, upon treatment with **1**, cGMP levels do not increase while this is a typical effect of NO release.[15] Moreover, nitrate esters of seven other NSAIDs induce considerably less apoptosis compared to **1**.[16] These conflicting results inspired us to probe the mechanism of action for **1** from a detailed molecular point of view by investigating a set of small-molecule analogues obtained through stepwise omission of the hybrid components. Toward this end, we used organic-chemical, computational, and biochemical approaches as well as ^{1}H and ^{15}N NMR spectroscopy. In this report, we disclose our surprising finding that the designer hybrid drug **1**, paradoxally, is not a hybrid drug after all.

Results and Discussion

Synthesis and Activity of Model Compounds. As previously reported, *meta*-isomer **2** is less active than its positional isomers (**1** and **3**) in inducing apoptosis in colon cancer cells.[5] This important finding suggests a crucial role for aromatic resonance interaction. Therefore, we selected model compounds having

both a *para*- or *meta*-substituted aromatic core. The general synthesis of these compounds, and of additional compounds discussed later in this paper, is outlined in Scheme 1. The appropriate hydroxybenzaldehyde was acylated with RCOOCl, and the resulting aldehyde was smoothly reduced with NaBH$_4$ in THF in good yields. The benzylic alcohol thus obtained was chlorinated with the aid of SOCl$_2$. A final substitution reaction with AgNO$_3$ in MeCN yielded the desired nitrate compounds. Initially, the selection of model compounds of **1** involved the replacement of the ASA-ester by an acetyl ester (**7a**) and of the nitrate moiety by an alcohol group (**5c**). Their activities were investigated by measuring the extent of cell death they induce in HT29 colon cancer cells after a 24 h incubation. As can be seen from Figure 1A, reference compounds ASA, *meta*-isomer **2**, and conventional NO-donor SNAP were less active than **1** in inducing cell death. In sharp contrast, acetyl ester **7a** is considerably more active than **1**, indicating that the ASA ester is not required and that a less bulky ester increases activity (Figure 1B). Replacement of the nitrate group by an alcohol

Table 1. Conversion and *S/O* Ratios for Investigated Compounds as Deduced from Diagnostic ArCH$_2$ ^{1}H NMR Signals[a]

cmpd				thiol	conversion[b] (%)	major adduct	*S/O* ratio
1	R = ASA	L = ONO$_2$	(*para*)	NAC	∼4	**19a**	>10[c]
2	R = ASA	L = ONO$_2$	(*meta*)	NAC	∼6	**11b**	0.49 ± 0.05
6c	R = ASA	L = Cl	(*para*)	NAC	∼6	**19a**	>10[c]
7a	R = Ac	L = ONO$_2$	(*para*)	NAC	100	**19a**	13.2 ± 1.7
7d	R = Ac	L = ONO$_2$	(*meta*)	NAC	100	**11b**	0.44 ± 0.04
6a	R = Ac	L = Cl	(*para*)	NAC	100	**19a**	17.0 ± 2.9
6a				GSH	100	**12**	>20[c]
15	R = Me	L = Cl	(*para*)	NAC	100	**11c**	0.15 ± 0.01

[a] Results are presented as the mean of three (for **6a**) or two (all others) experiments with the standard deviation given where appropriate. For exact yields and analytical characteristics of major adducts, see Supporting Information. [b] Most compounds reacted completely to give homogeneous mixtures. For **1**, **2**, and **6c**, the filtrates were used due to incomplete reaction owing to low solubility and slow ester hydrolysis. [c] A minimum *S/O* ratio was determined from NMR and LC-MS due to low product concentrations (**1**, **6c**) or complex NMR spectra (**6a** with GSH).

(**5c**) was detrimental for activity, a finding disclosed previously by others.[5] However, compared to an alcohol, the more electron-withdrawing nitrate group imposes a different chemical reactivity onto the neighboring carbon atom. This led us to recognize that the core skeletons of **1** and **7a** in fact satisfy the requirements for precursors to the class of *para*-QMs. The design of a few such precursors has been described,[17,18] and the major requirement is the presence of an aromatic ring substituted with both a masked phenolic group and a *para*-methylene group attached to a good leaving group L. QMs are highly electrophilic species and substituted QMs, naturally occurring as well, have been found to behave as cytotoxic agents by reacting with cellular nucleophiles such as GSH or DNA.[19−21] This led us to believe that compounds **1** and **7a** exert their activity by yielding a cytotoxic QM (**10**) in a similar fashion, with NO$_3^-$ as the leaving group (Scheme 2A).

Rate-determining hydrolysis of the carboxylic ester group, likely catalyzed by esterases, gives phenolate **8**, which at pH 7.4 can either reversibly bind a proton or it can rapidly and irreversibly undergo a 1,6-elimination,[18] with formation of QM **10** and the biologically inert nitrate ion. QM **10** represents the simplest *para*-QM conceivable. It has been studied before in P450 oxidations of *p*-cresol, where it is detected as a significant metabolite.[22] From those studies, it is known to react mostly with H$_2$O and cytoplasmic GSH yielding benzylalcohol **11a** and GSH-adduct **12**, respectively, the latter being the predominant product. This trapping of GSH by **10** to **12** is reported to lead to pronounced toxic effects.[22]

Mechanistic Studies on Quinone Methide Formation. QM formation from *para*-substituted benzylnitrates such as **1** and **7a** is a hitherto unknown transformation. We studied key steps in this process in theoretical and practical settings. To prove the role of the leaving group for the −ONO$_2$ moiety, similar molecules with a chloride atom as an alternative good leaving group (i.e., **6a−c** and **13**, see Schemes 1 and 2B) were studied as well. Linear transit calculations were conducted on the proton abstraction from phenols **9** and **13** by HO$^-$ ion using DFT[23] at the BLYP level. These calculations reveal that, upon deprotonation of phenols **9** and **13**, the resulting phenolates **8** and **14** at 37 °C undergo a rapid and energetically favorable [1,6]-elimination of the leaving group, thereby generating QM **10** (see Supporting Information for graph and details). In contrast, derivatives of **9** and **13** in which deprotonation of the phenol group is hindered by flanking *tert*-butyl groups are known to be stable and can be isolated.[24,25] All these observations indicate that phenol deprotonation is the actual trigger for release of **10** and that this will not occur as long as the phenol is protected by the ester group. Indeed, such rate-determining nature of the initial ester hydrolysis was confirmed by the observation that

hindered pivaloyl esters **6b** and **7b** were virtually untouched by aq methanol containing catalytic CF$_3$COOH, while their acetyl counterparts **6a** and **7a** quickly reacted at both the carboxylic ester and the benzylic group (see Supporting Information). The same results held true in aqueous medium at pH 7.4 and 37 °C, that is, **6b** and **7b** were stable, whereas **6a** and **7a** completely reacted to benzylic alcohol **11a** within hours (data not shown). These findings fully match previous reports on the differences in reactivity of analogous acetyl and pivaloyl esters with a phosphate leaving group.[26]

To investigate the reactivity profiles of the electrophilic species formed after carboxylic ester hydrolysis, a set of test compounds was incubated in D$_2$O (pD 7.4) at 37 °C in the presence of NAC (4 equiv) as a GSH model.[27] In these studies, dissolution and carboxylic ester hydrolysis are the slow steps, whereas any reactive electrophile formed will be trapped by either NAC or water, thereby providing a useful molecular in situ snapshot. Upon consumption of starting material (footnote *b*, Table 1), the mixtures were analyzed by ^{15}N NMR or by ^{1}H NMR, focusing on the shifts for the benzylic groups (Figure 2B,C). The NAC (**19a−c**)[28] and water (**11a−c**) conjugation products, the ratio of which is defined as the *S/O* ratio, accounted for >85% of products, except in the case of **15**, where the mass balance was 73%.[29] Noteworthy, no significant amounts of theoretically possible regioisomeric NAC addition products, such as resulting from direct addition to the ring of **10**, were observed by NMR nor LC-MS. Interestingly, the obtained *S/O* ratios (Table 1) can be clearly interpreted using the HSAB theory.[30] Compounds with a *para*-ester (**1**, **6c**, **7a**, **6a**) selectivity yielded NAC-adducts (*S/O* > 10, clearly visible in Figure 2B), whereas *meta*-esters (**2**, **7d**) preferentially yielded water-adducts (*S/O* < 1, clearly visible in Figure 2C). Interestingly, reaction of *para*-MeO-BnCl (**15**) via a S$_N$1 substitution through hard cation **16** gave an *S/O* ratio <0.2. This strongly suggests that direct S$_N$1 reaction of NAC or water with **9** through hard cation **17**, which is very similar to **16**, is not involved (Scheme 2A). In fact, these data further strengthen the case for soft QM **10** as reactive intermediate because it prefers thiols. The *meta* compounds, structurally not able to form QMs, preferentially react with water through S$_N$2 on phenol **18** while expelling the hard nitrate ion. Incubation of **6a** with GSH gave a slightly higher bias toward the S-adducts compared to NAC,[27] but analysis was complex due to extensive overlap of ^{1}H NMR signals. Last, ^{15}N-labeled **7a** (i.e., **20**) gave a single ^{15}N peak at 376.7 ppm (see Supporting Information), which corresponds to the ^{15}NO$_3^-$ ion. This confirms that nitrate only acts as a leaving group and that NO is not generated from thiols and **7a** at pH 7.4 (oxidation of liberated ^{15}NO in buffer leads to ^{15}NO$_2^-$ ions,[31] which would give a signal at 609 ppm[32]).

(A)

(B)

Cmpd			EC$_{50}$ (µM)
SNAP		-	>1,000
ASA		-	>1,000
1	R=ASA	L=ONO$_2$ (*para*)	106.7
2	R=ASA	L=ONO$_2$ (*meta*)	~1,000
5c	R=ASA	L=OH (*para*)	>1,000
7a	R=Ac	L=ONO$_2$ (*para*)	9.3
6c	R=ASA	L=Cl (*para*)	40.1
6a	R=Ac	L=Cl (*para*)	8.7

(C)

(D)
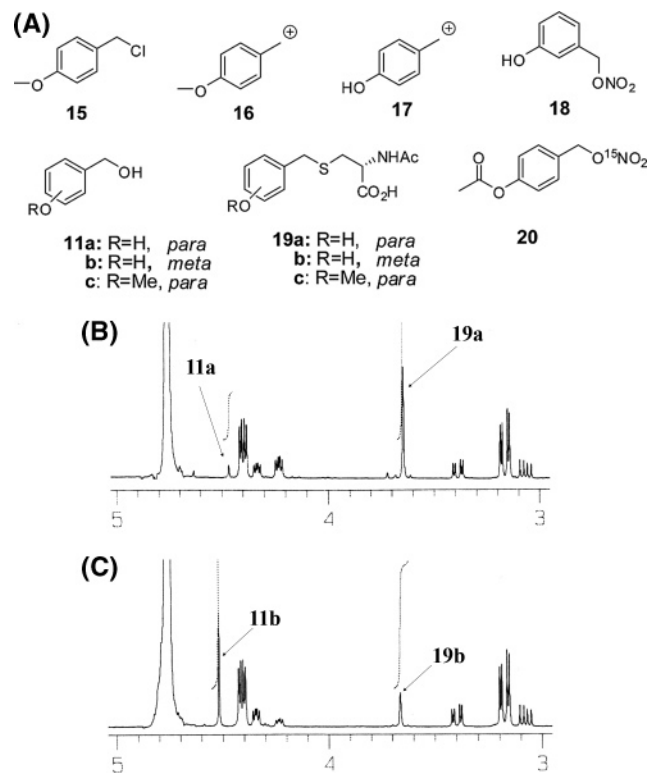
Figure 2. Differential reactivity of electrophilic species, formed after ester hydrolysis from selected compounds, toward water or NAC/GSH. (A) Relevant structures of intermediates involved. Note that exchangeable protons will be deuterated in the incubation studies of Table 1. (B,C) The 3.0–5.0 ppm regions of ^{1}H NMR spectra of fully completed incubations of compound **7a** (Figure 2B) and **7d** (Figure 2C) in D$_2$O. Clearly visible are the methylene groups (ArCH$_2$R) for the thioether adducts **19a,b** at 3.65 ppm and for hydrolysis products **11a,b** at 4.4 ppm. The large peak at 4.7 ppm is HOD. Integral curves for major adducts have been cropped to allow more visual detail.

Studies on the Apoptotic Activity of Quinone Methide. The discussed chemical studies clearly suggest that removal of one of the hybrid components from **1** (i.e., giving **6c** and **7a**) does not qualitatively change its chemical behavior toward cellular nucleophiles GSH and H$_2$O as all proceed through QM **10**. Interestingly, the same holds true for compound **6a** in which both hybrid components have been removed. We therefore speculated that all compounds with high *S/O* ratios exert apoptotic effects simply through the action of **10**. Indeed, while our work was in progress, others reported that apoptosis induction by NO-ASA involves GSH depletion,[13] thereby further substantiating the key role we hypothesized for QM **10**. To deliver definite proof for this hypothesis, the three key model compounds (**6c**, **7a**, and **6a**) were tested together with **1** and *meta*-NO-ASA (**2**) on HT29 cells in selected pharmacological studies. Figure 3A,B show the measured EC$_{50}$ values for all five compounds. Compound **6c** is about 2-fold more active than **1** in inducing cell death. More intriguingly, for **6a** and **7a**, this increase in apoptotic effect is a remarkable 10-fold. We attribute the latter to the higher sensitivity of small acetyl esters toward hydrolysis as compared to the bulkier ASA esters. Just as is the case for **1**, GSH depletion plays a key role in the case of cell death by **6a**, **6c**, and **7a** because intracellular GSH levels decreased significantly upon treatment with these compounds, whereas **2** did not induce this depletion (Figure 5A). Again, the small acetyl esters **6a** and **7a** are the most active. Another hallmark consequence of GSH depletion by NO-ASA is activation of caspase-3.[13] Indeed, **1**, **6c**, **7a**, and **6a** all induced cleavage of the typical caspase-3 substrate PARP, whereas, in
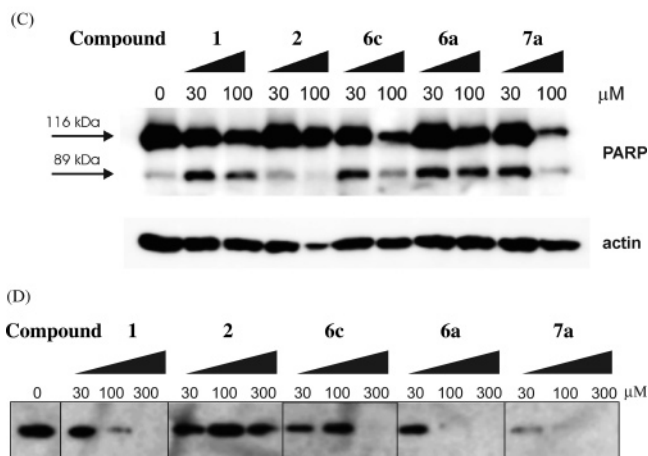
Figure 3. General pharmacological effects of key compounds **1**, **2**, **6c**, **7a**, and **6a** on colon cancer cells. (A) Induction of cell death on HT29 cells after 24 h. Cell death was measured using FACS with PI staining, and % living cells is plotted. Results are presented as the mean of 3–4 independent experiments, with bars depicting the standard errors. The value between parentheses represents the EC$_{50}$ value in µM for the respective compound. (B) Collected EC$_{50}$ values of all discussed compounds for induction of cell death on HT29 cells after 24 h. Standard deviations were all <10%. (C) Cleavage of PARP, 116 kDa, upon incubation of HT29 cells with varying concentrations of compound for 8 h, as measured by Western blot. (D) Cyclin D1 levels induced in SW480 cells after overnight starvation by serum treatment for 5 h in the absence or presence of varying concentrations of compounds.

contrast, **2** did not lead to significant PARP cleavage even at 300 µM (Figure 3C). The apoptotic pathway was investigated
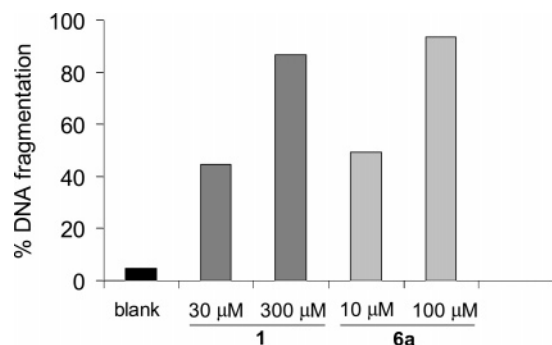
Figure 4. Extent of DNA fragmentation in HT29 cells induced by incubation with **1** (30 and 300 μM) or **6a** (10 and 100 μM) after 48 h, as measured by Nicoletti assay.

in further detail for **1** and **6a**. Both compounds induce DNA fragmentation in HT29 cells as measured with the Nicoletti assay (Figure 4). Furthermore, the apoptotic pathway induced by **1** and **6a** follows a typical mitochondrial-dependent mechanism. That is, Jurkat cells overexpressing Bcl-2 resist cell death induced by either compound and cell death induction was insensitive to the deletion of the adaptor molecule FADD (see Supporting Information). All these experiments clearly indicate that deletion of both the $-ONO_2$ group and ASA from **1** does not change the mechanism by which cell death is induced. Moreover, they confirm the notion that apoptotic features are induced by **6a** at lower concentrations than by **1**. It should be noted that GSH depletion can generally trigger both apoptosis and necrosis, depending on the circumstances.[33] We believe that at higher concentrations of our drugs, necrosis might be induced as indicated by low staining by an apoptosis-sensitive dye (data not shown), visual inspection of cell death, and decreasing intensity in Western blots (Figure 3C,D).

In addition to the discussed cytotoxic effects, compound **1** was also shown to induce cytostatic effects as it interferes with the interaction of β-catenin with Tcf in SW480 colon carcinoma cells.[13] We tested the serum-induced expression of cyclin D1, which is dependent on β-catenin/Tcf,[13] and found that inhibition of cyclin D1 induction is observed with **1**, **6a**, **6c**, and **7a**, while **2** is ineffective (Figure 3D).

The key GSH depletion through covalent adduct **12** was substantiated in more molecular detail for **1** and for **6a** (devoid of both ASA and $-ONO_2$ group). Pretreatment of HT29 cells with GSH-synthesis inhibitor BSO[34] increased the sensitivity of the cells toward cell death by **1** and **6a**, whereas replenishment with EtGSH[34] partially prevented this effect (Figure 5B). This reconfirms that GSH depletion is a major active contributor to the sequence leading to cell death. Previous metabolic studies on **1** only provided UV and MS evidence for key adduct **12**, but the lack of authentic **12** prevented unequivocal confirmation of the proposed molecular structure.[35] We synthesized **12** from GSH and **6a**, isolated it by LC-MS (55% extrapolated yield), and confirmed its structure by 2D-NMR and MS (Figure 5C and Supporting Information). The use of this standard enabled unequivocal assignment of **12** as the major GSH-QM adduct formed upon incubation of **1** or **6a** (both 100 μM) with HT29 cells (Figure 5D). The virtual absence of other peaks in the LC trace (detection at $m/z = 414$) strongly suggests that no other regioisomeric GSH adducts have been formed in the cell incubations, which is in accordance with the NAC incubation studies (vide supra). Lowering the drug concentration to 30 μM led to 4−5 times less **12** (see Supporting Information). All these observations underscore that the similarity of mode of action between **1** and **6a** starts at the basal molecular level by their
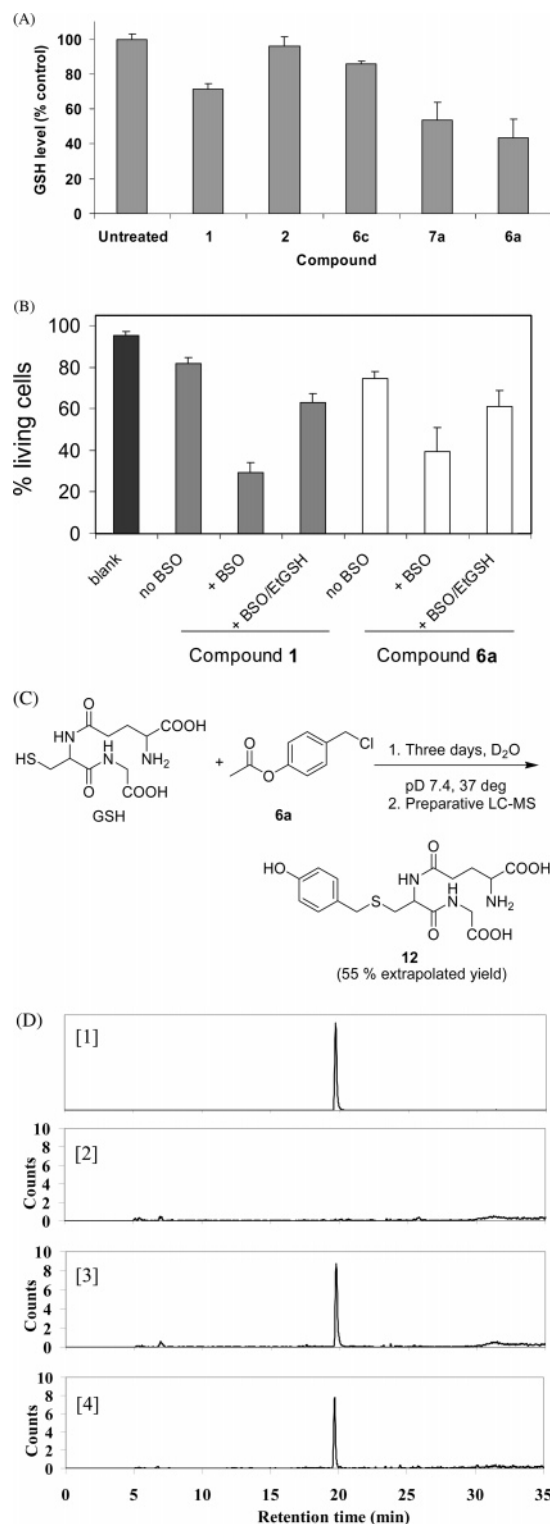

Figure 5. Confirmation of the specific role of GSH depletion in the apoptotic effects of key compounds **1**, **2**, **6c**, **7a**, and **6a**. (A) Effect on intracellular GSH levels after incubation of HT29 cells with 100 μM of compound for 1 h, as measured by Ellman's assay. Results are presented as the mean of three independent experiments, with bars depicting the standard deviations. (B) Induction of cell death of HT29 cells by **1** (50 μM) and **6a** (5 μM) without and with pretreatment with BSO or BSO followed by EtGSH. Cell death was measured using FACS with PI staining, and % living cells is plotted. Results are presented as the mean of four independent experiments, with bars depicting the standard deviations. (C) Synthesis of key adduct **12**. (D) LC-MS analysis with detection at $m/z = 414$ of [1] standard **12**, and of lysates of HT29 cells treated with [2] plain DMSO, [3] 100 μM of **1**, and [4] 100 μM of **6a**. The Y-axis represents counts in million.
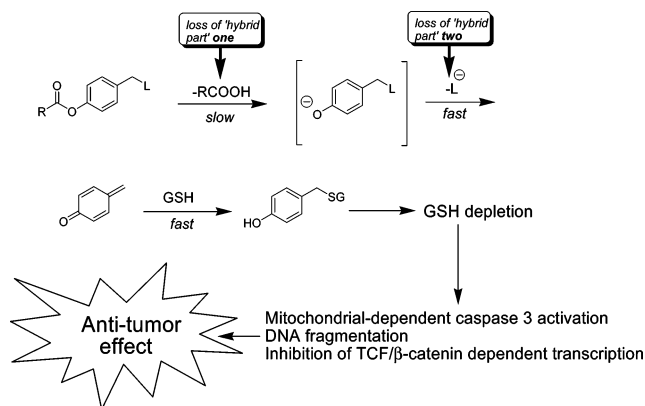
Figure 6. Overall mechanism of action for **1** and **6a** as well as for any other precursor to QM **10**. L = leaving group.

similar ability to provide a selective GSH-consuming metabolite (high S/O ratio), and this similarity is then amplified in downstream processes. Analogously, the lack of **2** to induce comparable cell death is a direct result of the lower chemical tendency of its metabolite (**18**) to bind GSH (low S/O ratio). Thus, hydrolysis of the phenolic ester triggers the chemical cascade, and the extent of GSH conjugation and the resulting apoptotic, necrotic, and transcriptional effects simply reflect the intrinsic physiochemical properties of the electrophiles formed immediately after carboxylic ester hydrolysis. That is, the cytotoxic species is formed from the chemical linker and not from any of the hybrid components. As such, this represents a major departure from the hybrid theory on which the design of **1** was based.[36] Last, we note that **1** has been specifically used as NO-donor in recent research.[37,38] Our results strongly suggest that such use may not be justified because under certain conditions **10** can be formed instead of NO.

Conclusion

The initial sequence of molecular events underlying the antitumor activity of an archetypical hybrid drug, i.e. preclinical candidate **1**, and the lack thereof for the *meta*-isomer **2**, have been elucidated and were shown to be almost completely dictated by the physical-organic HSAB principle. Remarkably, no role in the activity for NO or ASA was identified. Rather, the mechanism allows for the antitumor effect to be generalized to any phenyl ester possessing a *para*-methylene with a leaving group L (Figure 6). Thus, rate-determining carboxylic ester hydrolysis is followed by a rapid chain of events that ultimately leads to formation of an unsubstituted QM. This QM reacts with GSH, in response to which the cell initiates a variety of signaling pathways leading to cytotoxic and cytostatic effects. In their own right, any of such precursors to QM could be interesting for clinical purposes provided the carboxylic ester group is appropriately tuned toward localized cleavage. Equally important, the identification of the NO-donating group and ASA as passive bystanders and a quinone methide as the unexpected active agent should send out a clear warning signal to the promising field of hybrid drug research: caution should be exercised when selecting the (ideally) noninterfering spacer.

Experimental Section

Chemicals. Unless noted otherwise, all chemicals or reagents were purchased from Sigma-Aldrich. Growth medium consisted of IMDM (Cambrex) with 8% FCS (Cambrex, heated prior to use to deactivate esterases), glutamine (Cambrex), and Pen-Strep (Gibco). PI was purchased from Molecular Probes. Aprotinin and Lumilight were obtained from Roche, and leupeptin was from

Boehringer−Mannheim. Primary antibodies against PARP were purchased from Cell Signaling Technology, antibodies for actin were from Santa Cruz Biotechnology, antibodies for cyclin D1 were from BD Transduction Laboratories, and secondary HRP-linked swine-α-rabbit or goat-α-mouse antibodies were obtained from DAKO.

Computational Methods. All calculations were performed using ADF 2004.01.[23,39] A double-ζ core, triple-ζ valence, and doubly polarized basis set (TZ2P) was used. The Becke[40] exchange functional was used in combination with the LYP correlation functional[41] and ZORA relativistic corrections.[42] Calculations were performed in the gas phase or with inclusion of implicit solvent medium. The latter was carried out with the conductor-like screening model (COSMO) of salvation.[43,44] Equilibrium geometries were calculated, after which the linear transit method was applied to calculate the energies and geometries along the path obtained by hydroxide-mediated proton abstraction; the distance of the proton to the phenolic oxygen was increased from 1.1 Å to 3.0 Å in 30 steps. For the calculation of any energy barrier associated with the former process, the same linear transit method was applied but with stepwise increase of $ArCH_2$-L distance.

Cell Line. HT-29 or SW480 colon adenocarcinoma cells or Jurkat cells were used. Cells were counted using a cell counter from Bürker. Viability was determined by the trypan blue dye exclusion method.

Cell Death Assay by PI Exclusion. pEC50 Curves: Cells were seeded (25 000/well) and allowed to attach for 24 h. The supernatant was replaced by 1.0 mL medium pretreated with a DMSO solution of the compound (0−1000 μM, 5.0 μL). The final DMSO concentration for all experiments was 0.5%, except for the 600 μM experiment, where it was 1.0%. After 24 h of stimulation at 37 °C, the supernatant was collected and the cells were washed with PBS (400 μL) and detached with 400 μL TE (trypsin EDTA). The supernatant, PBS, and TE were centrifuged (1200 rpm for 5 min at 4 °C), and the supernatant was removed. Subsequently, the cells were treated with 50 μL BSA with PI (1:1000). After incubation for 10 min, the cells were analyzed for PI positivity by flow cytometry using the software "Cellquest". For each condition, 10 000 events were analyzed. Cells negative to PI were considered living and used for calculation of the EC_{50}, which was done with Prism software. **BSO/EtGSH Experiments:** Cells were seeded (25 000/well) and allowed to attach for 24 h. The supernatant was replaced by 1.0 mL medium with or without 200 μM BSO. After 4 h at 37 °C, the medium was removed and the cells were washed with warm PBS (1.0 mL). Subsequently, 0.5 mL of medium with or without EtGSH (10 mM) was added. After 3 h at 37 °C, the medium was removed and the cells were washed with warm PBS (1.0 mL). Then they were stimulated with the compounds and assayed as described above. **Jurkat-Bcl-2 Experiments:** Jurkat-neo or Bcl-2 transfectants were treated with the indicated concentrations of compound **1** and **6a** at a density of 1 million/mL for 20 h, and cell death was directly analyzed by PI as described above. **Fadd Experiments:** Jurkat clone JA3 or the corresponding FADD knockout clone (FADD−/−) were treated with anti-APO-1 (anti-Fas) to control for the efficacy of FADD deletion, as Fas-induced death completely depends on the presence of FADD, or with compound **1** and **6a**. After 20 h, cell death was analyzed using PI exclusion as described above.

DNA Fragmentation/Nicoletti Assay. HT29 cells were seeded at a density of 25 000/well and allowed to attach for 24 h. After this, the cells were treated with the indicated amount of compound **1** or **6a**. After 48 h, the cells were trypsinized and resuspended in Nicoletti buffer (0.1% Tx-100, 0.1% NaCitrate and 50 μg/mL PI). After overnight incubation at 4 °C, the DNA content of the remaining nuclei was determined using FACS and Cellquest software.

Cellular GSH Levels. GSH levels were determined using Ellman's reagent (5,5′-dithio-bis(2-nitrobenzoic acid, DTNB). In short, HT-29 cells were seeded in a 6-well plate (10^6 cells/well) in 2 mL of medium. After treatment with the different compounds for 1 h at 37 °C, cells were harvested, washed once with PBS, and

then lysed on ice in 40 μL of Triton X-100 lysis buffer without proteinase inhibitors. Lysates were cleared by centrifugation and intracellular GSH was measured in triplicate (10 μL of sample mixed with 50 μL of Ellman's reagent (0.5 mM DTNB) in HEPES buffer (0.5 M HEPES pH 7.5, 0.1 M NaCl, 0.05% Triton-X-100). The amount of GSH was quantified by measuring the absorbance at 405 nm in a microtiterplate reader (BioRad) and by using a standard curve of GSH. Percentages of GSH content from treated cells are compared to basal GSH content measured in untreated cells.

LC-MS Analysis of Cell Lysates. Equipment: A Shimadzu SCL-10A/Finnigan LC-QPeca with a Phenomenex Luna 5 μ C18 (150 × 4.60 mm, 5 μ) column was used, with the following gradient (A = 98.8% H_2O, 1% MeCN, and 0.2% HCOOH; B = 98.8% MeCN, 1% H_2O, and 0.2% HCOOH): 0 → 5 min, 0% B; 5 → 30 min, 0 → 100% B; 30 → 35 min, 100 → 0% B; 35 → 40 min, 0% B. The flow rate was 0.4 mL/min, and detection was conducted at m/z 414 (ionization: ESI, full MS, positive mode) or UV absorption at 254 nm. **Procedure:** Cells were seeded (1.2 × 10⁶/well) in 3 mL of medium and allowed to attach for 24 h. The supernatant was replaced by 1.8 mL of medium containing the compound in DMSO (final DMSO content 0.5%). For the blank, only DMSO was used. After 24 h of stimulation at 37 °C, the supernatant was collected and the well was washed with PBS (0.35 mL). To the mixed supernatant and washing, 250 μL of TE was added. After detachment of the cells, 750 μL of medium and 350 μL of 10% $HClO_4$ solution was added. The contents were mixed thoroughly by vortexing for 3 min, and high-molecular material was removed by sequential centrifugation (4000 rpm/20 min, then 14 000/15 min). The supernatant was immediately stored at −78 °C until analysis. Upon analysis, 20 μL was injected and the peak for **12** (at 19.8 min) was analyzed. Coinjection with authentic **12** was used to confirm peak identity, and amounts were calculated by using the mass areas for authentic **12**.

Supporting Information Available: Purity table, graph and additional details on computational chemistry, differences in reactivity between acetyl ester **7a** and pivaloyl ester **7b**, HPLC retention times and exact yields of the NAC incubation studies, detailed investigations on apoptotic pathway induced by **1** and **6a**, yields of adduct **12** in HT29 cell lysates, incubation of **20** with NAC, detailed synthetic procedures, protocols for NAC-incubation assays and Western blots, and full analytical data for all synthesized compounds. This material is available free of charge via the Internet at http://pubs.acs.org.

References

(1) Morphy, R.; Kay, C.; Rankovic, Z. From magic bullets to designed multiple ligands. *Drug Discovery Today* **2004**, *9*, 641−651.

(2) Bolla, M.; Almirante, N.; Benedini, F. Therapeutic potential of nitrate esters of commonly used drugs. *Curr. Top. Med. Chem.* **2005**, *88*, 707−720.

(3) Baron, J. A.; Cole, B. F.; Sandler, R. S.; Haile, R. W.; Ahnen, D.; Bresalier, R.; McKeown-Eyssen, G.; Summers, R. W.; Rothstein, R.; Burke, C. A.; Snover, D. C.; Church, T. R.; Allen, J. I.; Beach, M.; Beck, G. J.; Bond, J. H.; Byers, T.; Greenberg, E. R.; Mandel, J. S.; Marcon, N.; Mott, L. A.; Pearson, L.; Saibil, F.; van Stolk, R. U. A randomized trial of aspirin to prevent colorectal adenomas. *N. Engl. J. Med.* **2003**, *348*, 891−899.

(4) Williams, J. L.; Kashfi, K.; Ouyang, N.; del Soldato, P.; Kopelovich, L.; Rigas, B. NO-donating aspirin inhibits intestinal carcinogenesis in *Min* (APC^Min/+) mice. *Biochem. Biophys. Res. Comm.* **2004**, *313*, 784−788.

(5) Kashfi, K.; Borgo, S.; Williams, J. L.; Chen, J.; Gao, J.; Glekas, A.; Benedini, F.; del Soldato, P.; Rigas, B. Positional isomerism markedly affects the growth inhibition of colon cancer cells by nitric oxide-donating aspirin *in vitro* and *in vivo*. *J. Pharm. Exp. Ther.* **2005**, *312*, 978−988.

(6) Kashfi, K.; Ryann, Y.; Qiao, L. L.; Williams, J. L.; Chen, J.; Del Soldato, P.; Traganos, F.; Rigas, B. Nitric oxide-donating nonsteroidal anti-inflammatory drugs inhibit the growth of various cultured human cancer cells: Evidence of a tissue type-independent effect. *J. Pharm. Exp. Ther.* **2002**, *303*, 1273−1282.

(7) Huguenin, S.; Vacherot, F.; Fleury-Feith, F.; Riffaud, J-P.; Chopin, D. K.; Bolla, M.; Jaurand, M-C. Evaluation of the antitumoral potential of different nitric oxide-donating non-steroidal anti-inflammatory drugs (NO-NSAIDs) on human urological tumor cell lines. *Cancer Lett.* **2005**, *218*, 163−170.

(8) Tesei, A.; Ulivi, P.; Fabbri, F.; Rosetti, M.; Leonetti, C.; Scarsella, M.; Zupi, G.; Amadori, D.; Bolla, M.; Zoli, W. *In vitro* and *in vivo* evaluation of NCX 4040 cytotoxic activity in human colon cancer cell lines. *J. Transl. Med.* **2005**, *3*, 7−18.

(9) Hundley, T. R.; Rigas, B. Nitric oxide-donating aspirin inhibits colon cancer cell growth via mitogen-activated protein kinase activation. *J. Pharm. Exp. Ther.* **2006**, *316*, 25−34.

(10) Rosetti, M.; Tesei, A.; Ulivi, P.; Fabbri, F.; Vannini, I.; Brigliadori, G.; Amadori, D.; Bolla, M.; Zoli, W. Molecular characterization of cytotoxic and resistance mechanisms induced by NCX 4040, a novel NO-NSAID, in pancreatic cancer cell lines. *Apoptosis* **2006**, *11*, 1321−1330.

(11) Leonetti, C.; Scarsella, M.; Zupi, G.; Zoli, W.; Amadori, D.; Medri, L.; Fabbri, F.; Rosetti, M.; Ulivi, P.; Cecconetto, L.; Bolla, M.; Tesei, A. Efficacy of a nitric oxide−releasing nonsteroidal anti-inflammatory drug and cytotoxic drugs in human colon cancer cell lines *in vitro* and xenografts. *Mol. Cancer Ther.* **2006**, *5*, 919−926.

(12) Spiegel, A.; Hundley, T. R.; Chen, J.; Gao, J.; Ouyang, N.; Liu, X.; Go, M. F.; Tsioulias, G. J.; Kashfi, K.; Rigas, B. NO-donating aspirin inhibits both the expression and catalytic activity of inducible nitric oxide synthase in HT-29 human colon cancer cells. *Biochem. Pharm.* **2005**, *70*, 993−1000.

(13) Gao, J.; Liu, X.; Rigas, B. Nitric oxide-donating aspirin induces apoptosis in human colon cancer cells through induction of oxidative stress. *Proc. Natl. Acad. Sci. U.S.A.* **2005**, *102*, 17207−17212.

(14) Tanaka, T.; Kurose, A.; Halicka, H. D.; Huang, X.; Traganos, F.; Darzynkiewicz, Z. Nitrogen oxide-releasing aspirin induces histone H2AX phosphorylation, ATM activation and apoptosis preferentially in S-Phase cells. *Cell Cycle* **2006**, *5*, 1669−1674.

(15) Williams, J. L.; Nath, N.; Chen, J.; Hundley, J. R.; Gao, J.; Kopelovich, L.; Kashfi, K.; Rigas, B. Growth inhibition of human colon cancer cells by nitric oxide (NO)-donating aspirin is associated with cyclooxygenase-2 induction and β-catenin/T-Cell factor signaling, nuclear factor-κB, and NO synthase 2 inhibition: Implications for chemoprevention. *Cancer Res.* **2003**, *63*, 7613−7618.

(16) Yeh, R. K.; Chen, J.; Williams, J. L.; Baluch, M.; Hundley, T. R.; Rosenbaum, R. E.; Kalala, S.; Traganos, F.; Benardini, F.; del Soldato, P.; Kashfi, K.; Rigas, B. NO-donating nonsteroidal antiinflammatory drugs (NSAIDs) inhibit colon cancer cell growth more potently than traditional NSAIDs: a general pharmacological property? *Biochem. Pharm.* **2004**, *67*, 2197−2205.

(17) Dyer, R. G.; Turnbull, K. D. Hydrolytic stabilization of protected *p*-hydroxybenzyl halides designed as latent quinone methide precursors. *J. Org. Chem.* **1999**, *64*, 7988−7995.

(18) Wakselman, M. 1,6 and 1,4 eliminations from hydroxyl- and amino-substituted benzyl systems: Chemical and biochemical applications. *Nouv. J. Chem.* **1983**, *7*, 439−447.

(19) Thompson, D. C.; Thompson, J. A.; Sugumaran, M.; Moldéus, P. Biological and toxicological consequences of quinone methide formation. *Chem.-Biol. Interact.* **1992**, *86*, 129−162.

(20) Bolton, J. L.; Valerio, L. G., Jr.; Thompson, J. A. The enzymatic formation and chemical reactivity of quinone methides correlate with alkylphenol-induced toxicity in rat hepatocytes. *Chem. Res. Toxicol.* **1992**, *5*, 816−822.

(21) Kupchan, S. M.; Karim, A.; Marcks, C. Taxodione and Taxodone, two novel diterpenoid quinone methide tumor inhibitors from *Tuxodium distichum*. *J. Am. Chem. Soc.* **1968**, *90*, 5923−5924.

(22) Thompson, D. C.; Perera, K.; London, R. Quinone methide formation from *para* isomers of methylphenol (cresol), ethylphenol and isopropylphenol: Relationship to toxicity. *Chem. Res. Toxicol.* **1995**, *8*, 55−60.

(23) Te Velde, G.; Bickelhaupt, F. M.; Baerends, E. J.; Fonseca Guerra, C.; van Gisbergen, S. J. A.; Snijders, J. G.; Ziegler, T. Chemistry with ADF. *J. Comput. Chem.* **2001**, *22*, 931−967.

(24) Ronián, A.; Parker, V. D. Anodic oxidation of phenolic compounds. Part II. Products and mechanism of the anodic oxidation of hindered phenols. *J. Chem. Soc. C* **1971**, 3214−3218.

(25) Satgé de Caro, P.; Mouloungi, Z.; Gaset, A. Synthesis of derivatives of alkylamino alkyloxy propanol structures by *N*-alkylation, acylation, and nitration. Application as fuel additives. *J. Am. Oil Chem. Soc.* **1997**, *74*, 241−247.

(26) Mitchell, A. G.; Thornson, W.; Nicholls, D.; Irwin, W. J.; Freeman, S. Bioreversible protection for the phospho group: Bioactivation of the di(4-acyloxybenzyl) and mono(4-acyloxybenzyl) phosphoesters of methyl phosphonate and phosphonoacetate. *J. Chem. Soc., Perkin Trans. 1* **1992**, 2345−2353.

(27) GSH incubations were less useful as the diagnostic ArC*H₂*S group of **12** is buried under other GSH peaks and cannot be easily quantified. NAC and GSH behave similarly in conjugations of polysubstituted quinone methides, although GSH can be slightly more reactive. See, for example: Awad, H. M.; Boersma, M. G.; Boeren, S.; van Bladeren, P. J.; Vervoort, J.; Rietjens, I. M. C. M. Quenching of quercetin quinone/quinone methides by different thiolate scavengers: stability and reversibility of conjugate formation. *Chem. Res. Toxicol.* **2003**, *16*, 822−831.

(28) Reference adduct **19a** was obtained by reacting NAC with 4-hydroxybenzylalcohol in refluxing acetic acid.

(29) In the case of incubation of **15**, the most abundant products were the water adduct **11c** and, surprisingly, *N-N′*-di-*p*-OMe-benzylated cystine.

(30) Pearson, R. G. Hard and soft acids and bases. *J. Am. Chem. Soc.* **1963**, *85*, 3534−3539.

(31) Ignarro, L. J.; Fukuto, J. M.; Griscavage, J. M.; Rogers, N. E.; Byrns, R. E. Oxidation of nitric oxide in aqueous solution to nitrite but not nitrate: Comparison with enzymatically formed nitric oxide from *l*-arginine. *Proc. Natl. Acad. Sci. U.S.A.* **1993**, *90*, 8103−8107.

(32) Butler, A. R.; Rutherford, T. J.; Shorta, D. M.; Ridd, J. H. Tyrosine nitration and peroxonitrite (peroxynitrite) isomerisation: ¹⁵N CIDNP NMR Studies. *Chem. Commun.* **1997**, 669−670.

(33) Higuchi, Y. Glutathione depletion-induced chromosomal DNA fragmentation associated with apoptosis and necrosis. *J. Cell. Mol. Med.* **2004**, *8*, 455−464.

(34) Meurette, O.; Lefeuvre-Orfila, L.; Rebillard, A.; Lagadic-Gossmann, D.; Dimanche-Boitrel, M-T. Role of intracellular glutathione in cell sensitivity to the apoptosis induced by tumor necrosis factor α-related apoptosis-inducing ligand/anticancer drug combinations. *Clin. Cancer Res.* **2005**, *11*, 3075−3083.

(35) Gao, J.; Kashfi, K.; Rigas, B. *In vitro* metabolism of nitric oxide-donating aspirin: The effect of positional isomerism. *J. Pharm. Exp. Ther.* **2005**, *312*, 989−997.

(36) It should be mentioned that, by the time we were wrapping up this project after successfully proving the quinone methide theory, a WO patent (WO2005065361) became accessible in which one inventor of NO-ASA claims the use of NO-ASA as quinone methide precursor. However, this quinone methide has never been implicated in any of the many mechanistic studies on the effect of NO-ASA performed by the inventors.

(37) Mancina, R.; Filippi, S.; Marini, M.; Morelli, A.; Vignozzi, L.; Salonia, A.; Montorsi, F.; Mondaini, N.; Vannelli, G. B.; Donati, S.; Lotti, F.; Forti, G.; Maggi, M. Expression and functional activity of phosphodiesterase type 5 in human and rabbit vas deferens. *Mol. Hum. Reprod.* **2005**, *11*, 107−115.

(38) Morelli, A.; Filippi, S.; Mancina, R.; Luconi, M.; Vignozzi, L.; Marini, M.; Orlando, C.; Vannelli, B.; Aversa, A.; Natali, A.; Forti, G.; Giorgi, M.; Jannini, E. A.; Ledda, F.; Maggi, M. Androgens regulate phosphodiesterase type 5 expression and functional activity in corpora cavernosa. *Endocrinology* **2004**, *145*, 2253−2263.

(39) ADF2004.01, SCM; *Theoretical Chemistry*; Vrije Universiteit: Amsterdam, The Netherlands (http://www.scm.com).

(40) Becke, A. D. Density-functional exchange-energy approximation with correct asymptotic-behavior. *Phys. Rev. A: At., Mol., Opt. Phys.* **1988**, *38*, 3098−3100.

(41) Lee, C.; Yang, W.; Parr, R. G. Development of the Colle−Salvetti correlation-energy formula into a functional of the electron density. *Phys. Rev. B: Condens. Matter* **1988**, *37*, 785−789.

(42) van Lenthe, E.; Ehlers, A. E.; Baerends, E. Geometry optimizations in the zero order regular approximation for relativistic effects. *J. Chem. Phys.* **1999**, *110*, 8943−8953.

(43) Klamt, A.; Schüürmann, G. COSMO: A new approach to dielectric screening in solvents with explicit expressions for the screening energy and its gradient. *J. Chem. Soc., Perkin Trans. 2* **1993**, 799−805.

(44) Klamt, A. Conductor-like Screening Model for real solvents: A new approach to the quantitative calculation of solvation phenomena. *J. Phys. Chem.* **1995**, *99*, 2224−2235.